# Dynamically generated $N^*_{c\bar{c}}$ and $\Lambda^*_{c\bar{c}}$ resonances in the hidden charm sector around 4.3 GeV

R. Molina[1], J. J. Wu[2], E. Oset[3] and B. S. Zou[4]

[1]The George Washington University, Department of Physics, Columbian College of Arts & Sciences, 725 21st Street Nw, Washington, DC, 20052, USA. [2]Special Research Center for the Subatomic Structure of Matter (CSSM), School of Chemistry and Physics, University of Adelaide, Adelaide 5005, Australia. [3]Departamento de Física Teórica and IFIC, Centro Mixto Universidad de Valencia-CSIC, Institutos de Investigación de Paterna, Aptdo. 22085, 46071 Valencia, Spain. [4]Institute of High Energy Physics, CAS, P. O. Box 918(4), Beijing, 100049, China.

# Contents

1. Introduction: Pentaquark states
2. Formalism
   - The Local Hidden Gauge Lagrangian
   - Study of the vector(pseudoscalar) - baryon interaction in the hidden charm sector
3. Results: Dynamically generated $N^*_{c\bar{c}}$ or $(P_c)$ and $\Lambda^*_{c\bar{c}}$
4. Heavy Quark Spin Symmetry
5. Decay modes and quantum numbers of the $P_c$
6. Conclusions

# Introduction

- In 2015, the LHCb found two pentaquark states $P_c$ in $\Lambda_b^0 \to J/\psi K^- p$ decays. $M_1 = (4380 \pm 8 \pm 29)$ MeV, $\Gamma_1 = (205 \pm 18 \pm 86)$ MeV. $M_2 = (4449.8 \pm 1.7 \pm 2.5)$ MeV, $\Gamma_2 = (39 \pm 5 \pm 19)$ MeV.
- The possible quantum numbers assignments are $(3/2^-, 5/2^+)$, $(3/2^+, 5/2^-)$ or $(5/2^+, 3/2^-)$.
- These states could be also observed in $p\bar{p}$ collisions at PANDA or as enhancement in the $J/\psi N \to J/\psi N$ cross section.
- A purely pentaquark state, $N^*_{c\bar{c}}$, was predicted earlier (with similar mass and width to the $P_c(4450)$ in Phys. Rev. Lett 105, 232001(2010), Phys. Rev. C84, 015202(2011). J. J. Wu, R. Molina, E. Oset and B. S. Zou
- There can be similar states in the light sector. $N^*(1535)$ can be interpreted as bound state of $K\Sigma$, $K\Lambda$, and the two $\Lambda(1405)$'s as $\bar{K}N$ bound state and $\pi\Sigma$ resonance.

# Introduction

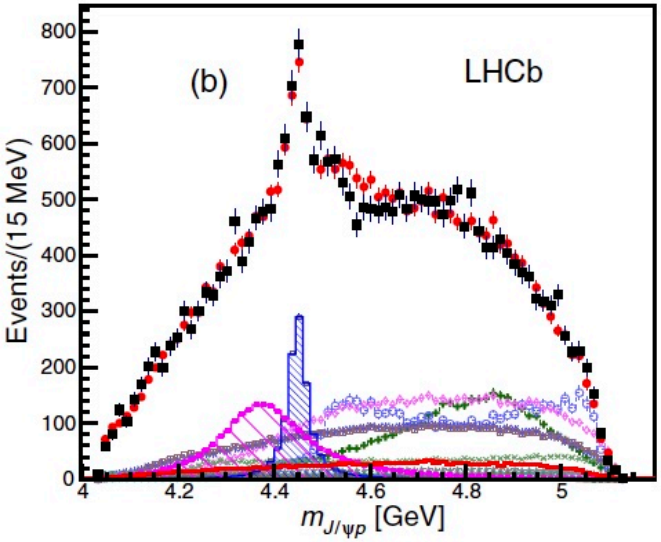


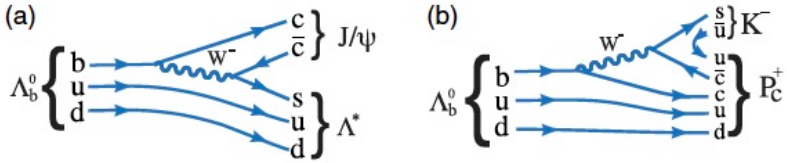


Figure 1. Left: Fit projection for (b) $m_{J/\psi p}$ for the reduced $\Lambda^*$ model with two $P_c^+$ states. The data are shown as solid (black) squares, while the solid (red) points show the result of the fit. The solid (red) histogram shows the background distribution. The (blue) open squares with the shaded histogram represent the $P_c^+(4450)^+$ state, and the shaded histogram topped with (purple) filled squares represents the $P_c(4380)^+$ state. Each $\Lambda^*$ component is also shown. The errors bars on the points showing the fit results are due to simulation statistics. Right: Feynman diagrams for (a) $\Lambda_b^0 \to J/\psi\Lambda^*$ and (b) $\Lambda_b^0 \to P_c^+ K^-$.

# The hidden gauge formalism

## Lagrangian (Bando,Kugo,Yamawaki)

$$\mathcal{L} = \mathcal{L}^{(2)} + \mathcal{L}_{III} \tag{1}$$

$$\begin{aligned} \mathcal{L}^{(2)} &= \frac{1}{4} f^2 \langle D_\mu U D^\mu U^\dagger + \chi U^\dagger + \chi^\dagger U \rangle \\ \mathcal{L}_{III} &= -\frac{1}{4} \langle V_{\mu\nu} V^{\mu\nu} \rangle + \frac{1}{2} M_V^2 \langle [V_\mu - \frac{i}{g} \Gamma_\mu]^2 \rangle \end{aligned} \tag{2}$$

$$D_\mu U = \partial_\mu U - ieQA_\mu U + ieUQA_\mu, \qquad U = e^{i\sqrt{2}P/f} \tag{3}$$

$$P \equiv \begin{pmatrix} \frac{1}{\sqrt{2}}\pi^0 + \frac{1}{\sqrt{6}}\eta_8 & \pi^+ & K^+ \\ \pi^- & -\frac{1}{\sqrt{2}}\pi^0 + \frac{1}{\sqrt{6}}\eta_8 & K^0 \\ K^- & \bar{K}^0 & -\frac{2}{\sqrt{6}}\eta_8 \end{pmatrix}, \qquad V_\mu \equiv \begin{pmatrix} \frac{1}{\sqrt{2}}\rho^0 + \frac{1}{\sqrt{2}}\omega & \rho^+ & K^{*+} \\ \rho^- & -\frac{1}{\sqrt{2}}\rho^0 + \frac{1}{\sqrt{2}}\omega & K^{*0} \\ K^{*-} & \bar{K}^{*0} & \phi \end{pmatrix}_\mu .$$

# VVP, PPV and BBV vertices

$$\mathcal{L}_{III} = -\frac{1}{4}\langle V_{\mu\nu}V^{\mu\nu}\rangle \longrightarrow \mathcal{L}_{III}^{(3V)} = ig\langle(\partial_\mu V_\nu - \partial_\nu V_\mu)V^\mu V^\nu\rangle$$

$$\downarrow$$

Bando, Kugo, Yamawaki

$$\vec{k} \simeq 0,\ \mathcal{L}_{III}^{(3V)} = ig\langle V^\mu\,[V_\nu, \partial_\mu V^\nu]\rangle$$

$$\mathcal{L}^{(2)} = \frac{1}{4}f^2\langle D_\mu U D^\mu U^\dagger\rangle \longrightarrow \mathcal{L}_{III}^{(PPV)} = -ig\langle V^\mu\,[P, \partial_\mu P]\rangle$$

Klingl, Kaiser, Weise

$$\mathcal{L}_{BBV} = g(\langle\bar{B}\gamma_\mu\,[V^\mu, B]\rangle + \langle\bar{B}\gamma_\mu B\rangle\langle V^\mu\rangle)$$

$$g = \frac{M_V}{2f}$$

# $PB$ and $VB$ resonances in the hidden charm sector

- $I = 1/2, S = 0$. Channels: (PB) $\bar{D}\Sigma_c$, $\bar{D}\Lambda_c^+$.
  (VB) $\bar{D}^*\Sigma_c$, $\bar{D}^*\Lambda_c^+$
- $I = 0, S = -1$. Channels: (PB) $\bar{D}_s\Lambda_c^+$, $\bar{D}\Xi_c$, $\bar{D}\Xi_c'$.
  (VB) $\bar{D}_s^*\Lambda_c^+$, $\bar{D}^*\Xi_c$, $\bar{D}^*\Xi_c'$

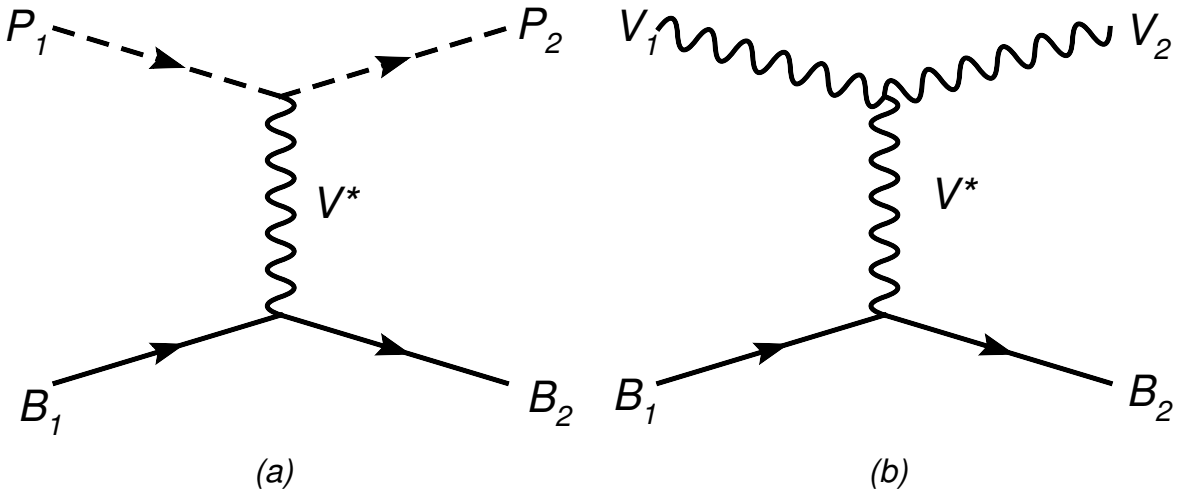


- $V^*$=$\rho$, $\omega$ in the $I = 1/2, S = 0$ sector, and $\rho, \omega, K^*$ in the $I = 0, S = -1$ sector.

## Evaluation of the amplitudes $P(V)B \to P(V)B$

Clebsh Gordan coefficients in SU(4):

$$\begin{aligned} PPV, 3V: &\quad 15 \otimes 15 = 15_F + 15_D + 1 + ..., \\ BBV: &\quad 20' \otimes 20' = 15_1 + 15_2 + 1 + ... \end{aligned} \tag{4}$$

$$t_{P_1P_2V} = g_{15_F} C_{15_F}(15 \otimes 15)\,(q_1 + q_2)_\mu \epsilon^\mu \tag{5}$$

$$\begin{aligned} t_{B_1\bar{B}_2V} = &\{g_{15_1}\, C_{15_1}(20' \otimes \bar{20}') + g_{15_2}\, C_{15_2}(20' \otimes \bar{20}') + \\ &g_1\, C_1(20' \otimes \bar{20}')\}\bar{u}_{r'}(p_2)\gamma \cdot \epsilon\, u_r(p_1) \end{aligned} \tag{6}$$

with $g_{15_F} = -2\sqrt{2}g$ and the reduced matrix elements, $g_{15_1}$, $g_{15_2}$ and $g_1$ are evaluated demanding:

1) The coupling $p\bar{p} \to J/\psi$ should be zero by OZI rules,
2) The coupling $p\bar{p} \to \phi$ should be zero by OZI rules,
3) The coupling $p\bar{p} \to \rho^0$ should be the one obtained in SU(3).

$$g_{15_1} = -g; \qquad g_{15_2} = 2\sqrt{3}\,g; \qquad g_1 = 3\sqrt{5}\,g\,. \tag{7}$$

## Evaluation of the amplitudes $P(V)B \to P(V)B$

- The transition potential from the (light) vector-meson ($\rho$, $\omega$, $K^*$)-exchange diagram is given by

$$V_{ab(P_1B_1 \to P_2B_2)} = \frac{C_{ab}}{4f^2}(q_1^0 + q_2^0), \tag{8}$$

$$V_{ab(V_1B_1 \to V_2B_2)} = \frac{C_{ab}}{4f^2}(q_1^0 + q_2^0)\vec{\epsilon}_1 \cdot \vec{\epsilon}_2 \ , \tag{9}$$

| | $\bar{D}^*\Sigma_c$ | $\bar{D}^*\Lambda_c^+$ |
|---|---|---|
| $\bar{D}^*\Sigma_c$ | $-1$ | $0$ |
| $\bar{D}^*\Lambda_c^+$ | | $1$ |

Table 1. Coefficients $C_{ab}$ in the sectors $I = 1/2$, $S = 0$.

| | $\bar{D}_s^*\Lambda_c^+$ | $\bar{D}^*\Xi_c$ | $\bar{D}^*\Xi_c'$ |
|---|---|---|---|
| $\bar{D}_s^*\Lambda_c^+$ | $0$ | $-\sqrt{2}$ | $0$ |
| $\bar{D}^*\Xi_c$ | | $-1$ | $0$ |
| $\bar{D}^*\Xi_c'$ | | | $-1$ |

Table 2. Coefficients $C_{ab}$ in the $I = 0$, $S = -1$ sector.

# Unitarization procedure and search for poles

## Bethe-Salpeter equation

$$T = [I - VG]^{-1} V \tag{10}$$

Meson-baryon loop function $G$:s

$$G = i2M \int \frac{d^4q}{(2\pi)^4} \frac{1}{q^2 - m^2 + i\epsilon} \frac{1}{(P-q)^2 - M^2 + i\epsilon} \ , \tag{11}$$

which upon using dimensional regularization can be recast as

$$\begin{aligned} G \quad = \quad & \frac{2M}{16\pi^2} \{ a + \mathrm{Log} \frac{M^2}{\mu^2} + \frac{m^2 - M^2 + s}{2s} \mathrm{Log} \frac{m^2}{M^2} \\ & + \frac{p}{\sqrt{s}} \Big( \mathrm{Log} \frac{s - M^2 + m^2 + 2p\sqrt{s}}{-s + M^2 - m^2 + 2p\sqrt{s}} + \mathrm{Log} \frac{s + M^2 - m^2 + 2p\sqrt{s}}{-s - M^2 + m^2 + 2p\sqrt{s}} \Big) \} \ , \end{aligned} \tag{12}$$

where P is the total four-momentum of the system, $p$ is the three-momentum of the meson in the center of mass frame

$$p = \frac{1}{2\sqrt{s}} \sqrt{(s - (m_1 + m_2)^2)(s - (m_1 - m_2))^2} \tag{13}$$

# Unitarization procedure and search for poles

## Second Riemann sheet

To find resonances from the scattering matrix we go to the second Riemann sheet in the complex plane where the T matrix develops poles associated to these states. For a complex $\sqrt{s}$ in the second Riemann sheet,

$$G_l^{II}(\sqrt{s}) = G_l^{I}(\sqrt{s}) + i\frac{q}{4\pi\sqrt{s}} \ , \tag{14}$$

with $Im(q) > 0$.

- Bound states appear below threshold while resonances are identified with poles above threshold in the second Riemann Sheet.
- The coupling of the state to the pseudoscalar (vector)-baryon component can be evaluated as

$$T_{ab} = \frac{g_a g_b}{\sqrt{s} - z_R} \tag{15}$$

# Results

Bound states with a binding energy $30 - 100$ MeV are found in the $I = 1/2$ ($J = 1/2, 3/2$) sector. In the $I = 3/2$ sector the interaction is repulsive.

| $(I, S)$ | $\alpha = -2.2$ | $\alpha = -2.3$ | $\alpha = -2.4$ |
|---|---|---|---|
| $(1/2, 0)$ | 4291 | 4269 | 4240 |
| $(0, -1)$ | 4247 | 4213 | 4170 |
| | 4422 | 4403 | 4376 |

Table 3. Pole position $z_R$ from $PB \to PB$ using the two different $G$ functions with dim. reg. and cutoff (MeV).

| $(I, S)$ | $\alpha = -2.2$ | $\alpha = -2.3$ | $\alpha = -2.4$ |
|---|---|---|---|
| $(1/2, 0)$ | 4438 | 4418 | 4391 |
| $(0, -1)$ | 4399 | 4370 | 4330 |
| | 4568 | 4550 | 4526 |

Table 4. Pole position $z_R$ from $VB \to VB$ using the two different $G$ functions with dim. reg. and cutoff (MeV).

| $(I, S)$ | $z_R$ (MeV) | $g_a$ | | |
|---|---|---|---|---|
| $(1/2, 0)$ | | $\bar{D}\Sigma_c$ | $\bar{D}\Lambda_c^+$ | |
| | 4269 | 2.85 | 0 | |
| $(0, -1)$ | | $\bar{D}_s\Lambda_c^+$ | $\bar{D}\Xi_c$ | $\bar{D}\Xi_c'$ |
| | 4213 | 1.37 | 3.25 | 0 |
| | 4403 | 0 | 0 | 2.64 |

Table 5. Pole position $z_R$ and coupling constants $g_a$ for the states from $PB \to PB$.

| $(I, S)$ | $z_R$ (MeV) | $g_a$ | | |
|---|---|---|---|---|
| $(1/2, 0)$ | | $\bar{D}^*\Sigma_c$ | $\bar{D}^*\Lambda_c^+$ | |
| | 4418 | 2.75 | 0 | |
| $(0, -1)$ | | $\bar{D}_s^*\Lambda_c^+$ | $\bar{D}^*\Xi_c$ | $\bar{D}^*\Xi_c'$ |
| | 4370 | 1.23 | 3.14 | 0 |
| | 4550 | 0 | 0 | 2.53 |

Table 6. Pole position $z_R$ and coupling constants $g_a$ for the states from $VB \to VB$.

Similar results are obtained integrating $G_{P(V)B}$ with $\Lambda = 700 - 900$ MeV.

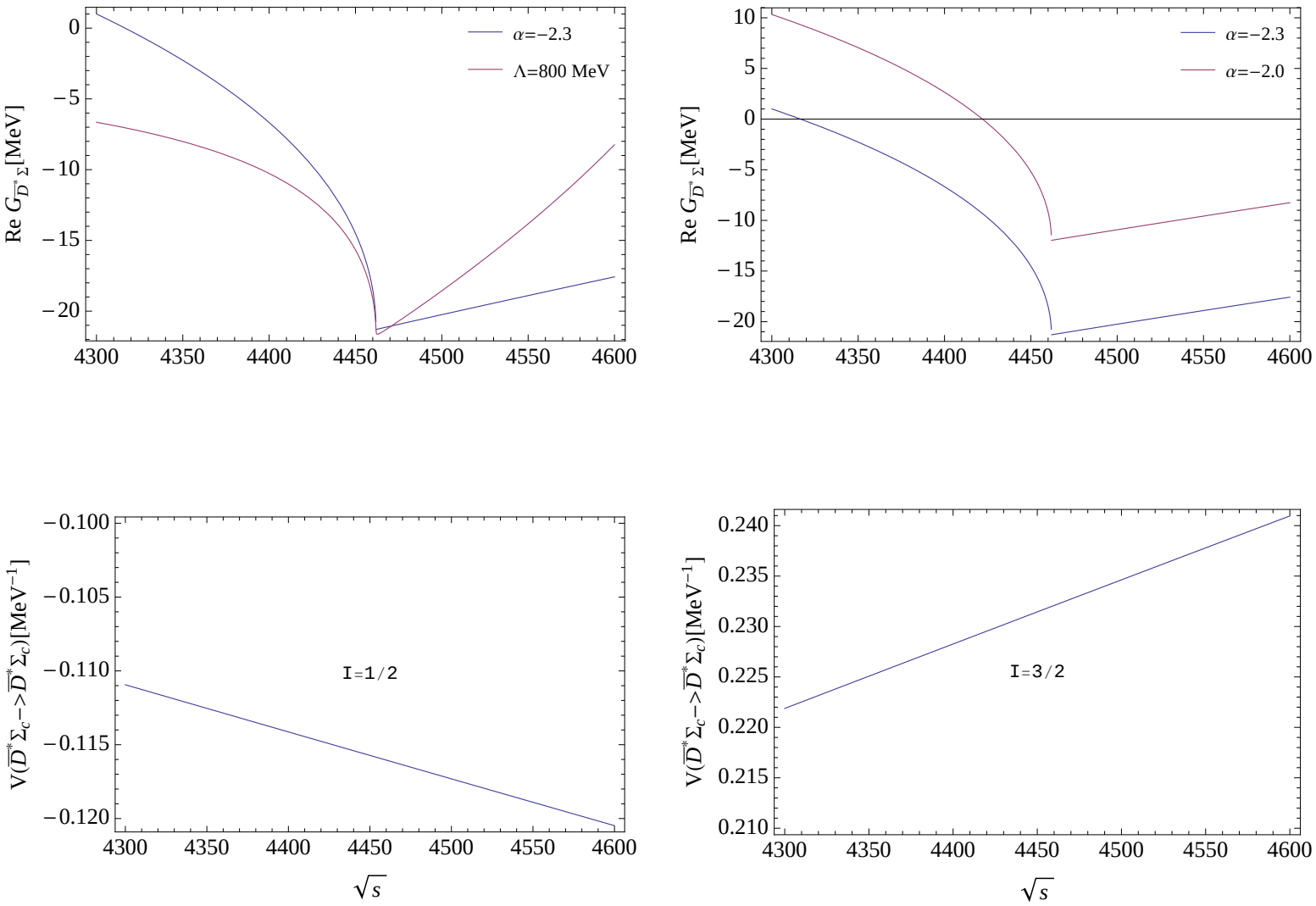

# Results including $\eta_c N$, $\eta_c \Lambda$, $J/\psi N$, $J/\Lambda$ $\left(V(PB \to \eta_c B) = -\frac{C g^2}{p_{D^*}^2 - M_{D^*}^2}(E_P + E_{\eta_c})\right)$

| $(I,S)$ | $z_R$ (MeV) | $g_a$ | | | |
|---|---|---|---|---|---|
| $(1/2,0)$ | | $\bar{D}\Sigma_c$ | $\bar{D}\Lambda_c^+$ | $\eta_c N$ | |
| | $4265-11.6i$ | 2.97 | 0.10 | 0.94 | |
| $(0,-1)$ | | $\bar{D}_s\Lambda_c^+$ | $\bar{D}\Xi_c$ | $\bar{D}\Xi_c'$ | $\eta_c\Lambda$ |
| | $4210-2.9i$ | 1.42 | 3.28 | 0.19 | 0.57 |
| | $4398-8.0i$ | 0.01 | 0.06 | 2.75 | 0.74 |

Table 7. Pole position, $z_R$ and coupling constants, $g_a$, to various channels for the states from $PB \to PB$ including the $\eta_c N$ and $\eta_c \Lambda$ channel.

| $(I,S)$ | $z_R$ | $g_a$ | | | |
|---|---|---|---|---|---|
| $(1/2,0)$ | | $\bar{D}^*\Sigma_c$ | $\bar{D}^*\Lambda_c^+$ | $J/\psi N$ | |
| | $4415-9.5i$ | 2.83 | 0.08 | 0.85 | |
| $(0,-1)$ | | $\bar{D}_s^*\Lambda_c^+$ | $\bar{D}^*\Xi_c$ | $\bar{D}^*\Xi_c'$ | $J/\psi\Lambda$ |
| | $4368-2.8i$ | 1.27 | 3.16 | 0.16 | 0.47 |
| | $4547-6.4i$ | 0.01 | 0.05 | 2.61 | 0.61 |

Table 8. Pole position, $z_R$ and coupling constants, $g_a$, to various channels for the states from $VB \to VB$ including the $J/\psi N$ and $J/\psi\Lambda$ channel.

# Decay modes

- $I = 1/2, S = 0.$
  (PB) $\bar{D}\Sigma_c$, $\bar{D}\Lambda_c^+$ $\eta_c N$: $\pi N$, $\eta N$, $\eta' N$, $K\Sigma$, $K\Lambda$
  (VB) $\bar{D}^*\Sigma_c$, $\bar{D}^*\Lambda_c^+$, $J/\psi N$: $\rho N$, $\omega N$, $K^*\Sigma$, $K^*\Lambda$
- $I = 0, S = -1.$
  (PB) $\bar{D}_s\Lambda_c^+$, $\bar{D}\Xi_c$, $\bar{D}\Xi_c'$, $\eta_c\Lambda$: $\pi\Sigma$, $\eta\Lambda$, $\eta'\Lambda$, $\bar{K}N$, $K\Xi$
  (VB) $\bar{D}_s^*\Lambda_c^+$, $\bar{D}^*\Xi_c$, $\bar{D}^*\Xi_c'$, $J/\psi\Lambda$: $\bar{K}^*N$, $\rho\Sigma$, $\omega\Lambda$, $\phi\Lambda$, $K^*\Xi$

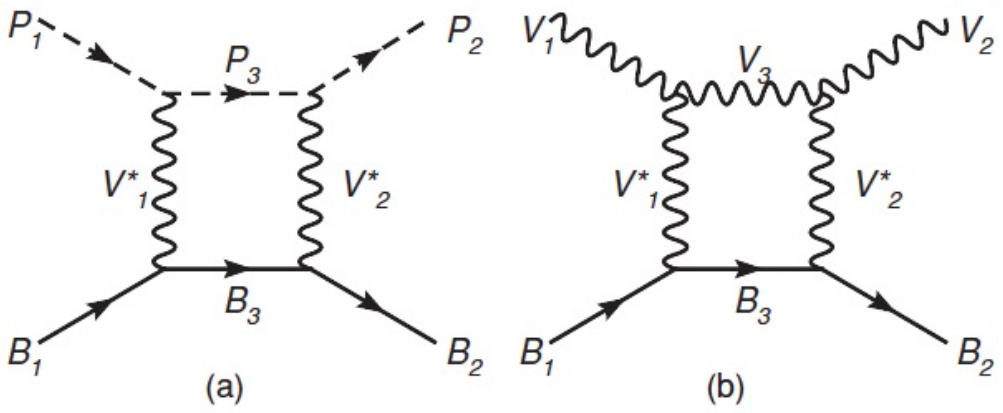


The $D^*$- exchange is supressed compared to the $\rho$, $\omega$ exchange due to the factor $\simeq m_\rho^2/m_{D^*}^2 \simeq 0.15$.

# Results

## Prediction of narrow $N^*$ and $\Lambda^*$ resonances above 4.2 GeV

| $(I,S)$ | $M$ | $\Gamma$ | $\Gamma_i$ | | | | | |
|---|---|---|---|---|---|---|---|---|
| $(1/2,0)$ | | | $\pi N$ | $\eta N$ | $\eta' N$ | $K\Sigma$ | | $\eta_c N$ |
| | 4261 | 56.9 | 3.8 | 8.1 | 3.9 | 17.0 | | 23.4 |
| $(0,-1)$ | | | $\bar{K}N$ | $\pi\Sigma$ | $\eta\Lambda$ | $\eta'\Lambda$ | $K\Xi$ | $\eta_c\Lambda$ |
| | 4209 | 32.4 | 15.8 | 2.9 | 3.2 | 1.7 | 2.4 | 5.8 |
| | 4394 | 43.3 | 0 | 10.6 | 7.1 | 3.3 | 5.8 | 16.3 |

Table 9. Mass and width of the PB resonances (units in MeV).

| $(I,S)$ | $M$ | $\Gamma$ | $\Gamma_i$ | | | | | |
|---|---|---|---|---|---|---|---|---|
| $(1/2,0)$ | | | $\rho N$ | $\omega N$ | $K^*\Sigma$ | | | $J/\psi N$ |
| | 4412 | 47.3 | 3.2 | 10.4 | 13.7 | | | 19.2 |
| $(0,-1)$ | | | $\bar{K}^*N$ | $\rho\Sigma$ | $\omega\Lambda$ | $\phi\Lambda$ | $K^*\Xi$ | $J/\psi\Lambda$ |
| | 4368 | 28.0 | 13.9 | 3.1 | 0.3 | 4.0 | 1.8 | 5.4 |
| | 4544 | 36.6 | 0 | 8.8 | 9.1 | 0 | 5.0 | 13.8 |

Table 10. Mass and width of the VB resonances.

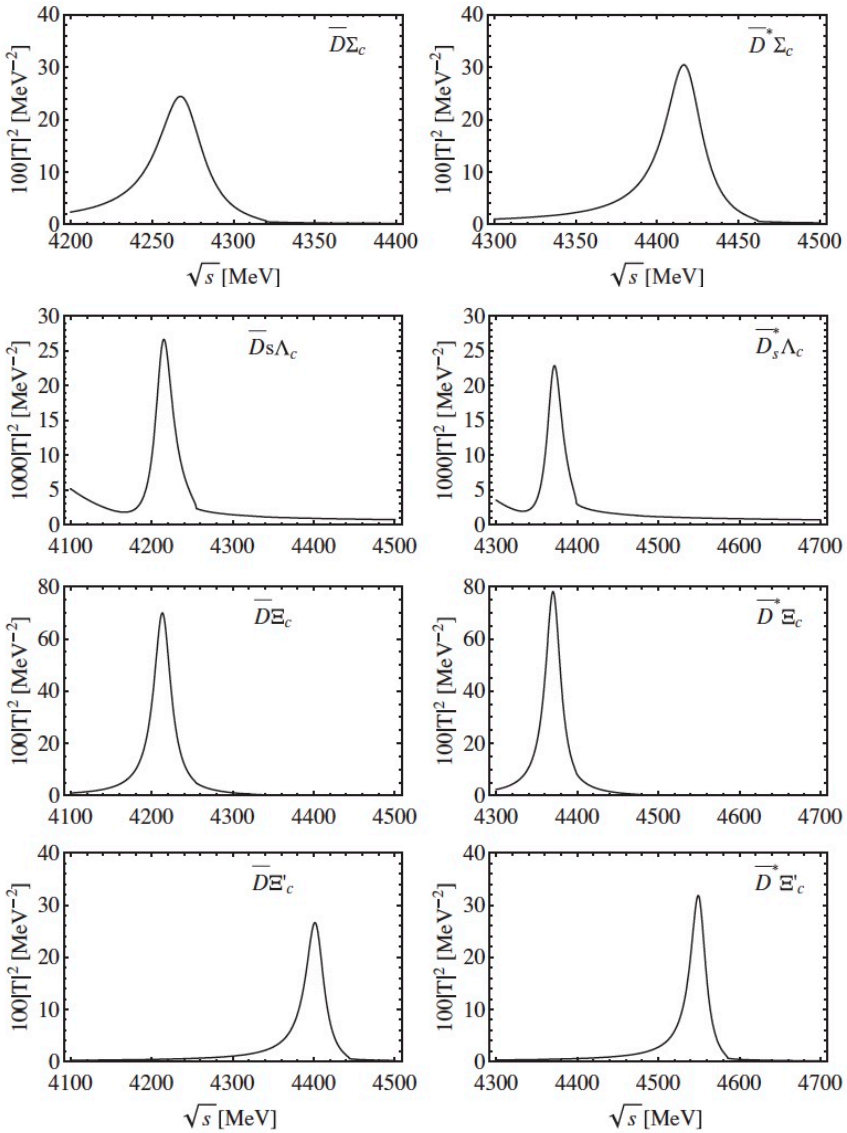
$\bar{D}\Sigma_c$
$\bar{D}^*\Sigma_c$
$\bar{D}s\Lambda_c$
$\bar{D}_s^*\Lambda_c$
$\bar{D}\Xi_c$
$\bar{D}^*\Xi_c$
$\bar{D}\Xi'_c$
$\bar{D}^*\Xi'_c$
$100|T|^2$ [MeV$^{-2}$]
$1000|T|^2$ [MeV$^{-2}$]
$\sqrt{s}$ [MeV]

# Production cross section of the $N^*$ resonances at FAIR

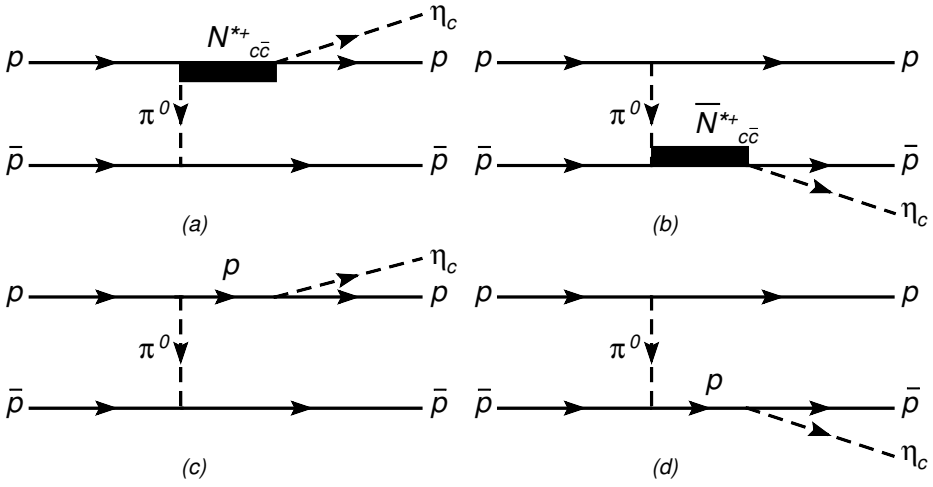


- $\bar{p}$ beam of $15$ GeV/c, $\sqrt{s} = 5470$ MeV $\rightarrow M_X \simeq 4538$ MeV. $\frac{d\sigma_{p\bar{p}\rightarrow N^{*+}_{c\bar{c}}(4265)\bar{p}\rightarrow\eta_c p\bar{p}}}{dcos\theta dM_I^2} = 0.3\,\mu b/GeV^2$ at peak, $\sigma \simeq 0.07\,\mu b$.
- $\sigma(p\bar{p} \rightarrow N^{*+}_{c\bar{c}}(4418)\bar{p} \rightarrow \eta_c p\bar{p}) \simeq 0.002\mu b$.

This corresponds to an event production rate of $80000$ and $1700$ events per day for the $N^{*+}_{c\bar{c}}(4265)$ and $N^{*+}_{c\bar{c}}(4418)$ respectively for a Luminosity of $10^{31} cm^{-2} s^{-1}$.

# Heavy Quark Spin Symmetry

- The spin-dependendent interactions are proportional to the chromomagnetic moment of the heavy quark, being of the order of $1/m_Q$.
- In a HQSS basis, $|S_{c\bar{c}}, \mathcal{L}, J, \alpha\rangle_{(l_M, l_B)}$, and with the dynamics of the hidden gauge Lagrangian, one gets, $\lambda_2 = \mu_3$. C. W. Xiao, J. Nieves and E. Oset, PRD88,056012 (2013)

| | $\eta_c N$ | $J_\Psi N$ | $\bar{D}\Lambda_c$ | $\bar{D}\Sigma_c$ | $\bar{D}^*\Lambda_c$ | $\bar{D}^*\Sigma_c$ | $\bar{D}^*\Sigma_c^*$ |
|---|---|---|---|---|---|---|---|
| $\eta_c N$ | $\mu_1$ | $0$ | $\frac{\mu_{12}}{2}$ | $\frac{\mu_{13}}{2}$ | $\frac{\sqrt{3}\mu_{12}}{2}$ | $-\frac{\mu_{13}}{2\sqrt{3}}$ | $\sqrt{\frac{2}{3}}\mu_{13}$ |
| $J_\Psi N$ | $0$ | $\mu_1$ | $\frac{\sqrt{3}\mu_{12}}{2}$ | $-\frac{\mu_{13}}{2\sqrt{3}}$ | $-\frac{\mu_{12}}{2}$ | $\frac{5\mu_{13}}{6}$ | $\frac{\sqrt{2}\mu_{13}}{3}$ |
| $\bar{D}\Lambda_c$ | $\frac{\mu_{12}}{2}$ | $\frac{\sqrt{3}\mu_{12}}{2}$ | $\mu_2$ | $0$ | $0$ | $\frac{\mu_{23}}{\sqrt{3}}$ | $\sqrt{\frac{2}{3}}\mu_{23}$ |
| $\bar{D}\Sigma_c$ | $\frac{\mu_{13}}{2}$ | $-\frac{\mu_{13}}{2\sqrt{3}}$ | $0$ | $\frac{1}{3}(2\lambda_2+\mu_3)$ | $\frac{\mu_{23}}{\sqrt{3}}$ | $\frac{2(\lambda_2-\mu_3)}{3\sqrt{3}}$ | $\frac{1}{3}\sqrt{\frac{2}{3}}(\mu_3-\lambda_2)$ |
| $\bar{D}^*\Lambda_c$ | $\frac{\sqrt{3}\mu_{12}}{2}$ | $-\frac{\mu_{12}}{2}$ | $0$ | $\frac{\mu_{23}}{\sqrt{3}}$ | $\mu_2$ | $-\frac{2\mu_{23}}{3}$ | $\frac{\sqrt{2}\mu_{23}}{3}$ |
| $\bar{D}^*\Sigma_c$ | $-\frac{\mu_{13}}{2\sqrt{3}}$ | $\frac{5\mu_{13}}{6}$ | $\frac{\mu_{23}}{\sqrt{3}}$ | $\frac{2(\lambda_2-\mu_3)}{3\sqrt{3}}$ | $-\frac{2\mu_{23}}{3}$ | $\frac{1}{9}(2\lambda_2+7\mu_3)$ | $\frac{1}{9}\sqrt{2}(\mu_3-\lambda_2)$ |
| $\bar{D}^*\Sigma_c^*$ | $\sqrt{\frac{2}{3}}\mu_{13}$ | $\frac{\sqrt{2}\mu_{13}}{3}$ | $\sqrt{\frac{2}{3}}\mu_{23}$ | $\frac{1}{3}\sqrt{\frac{2}{3}}(\mu_3-\lambda_2)$ | $\frac{\sqrt{2}\mu_{23}}{3}$ | $\frac{1}{9}\sqrt{2}(\mu_3-\lambda_2)$ | $\frac{1}{9}(\lambda_2+8\mu_3)$ |

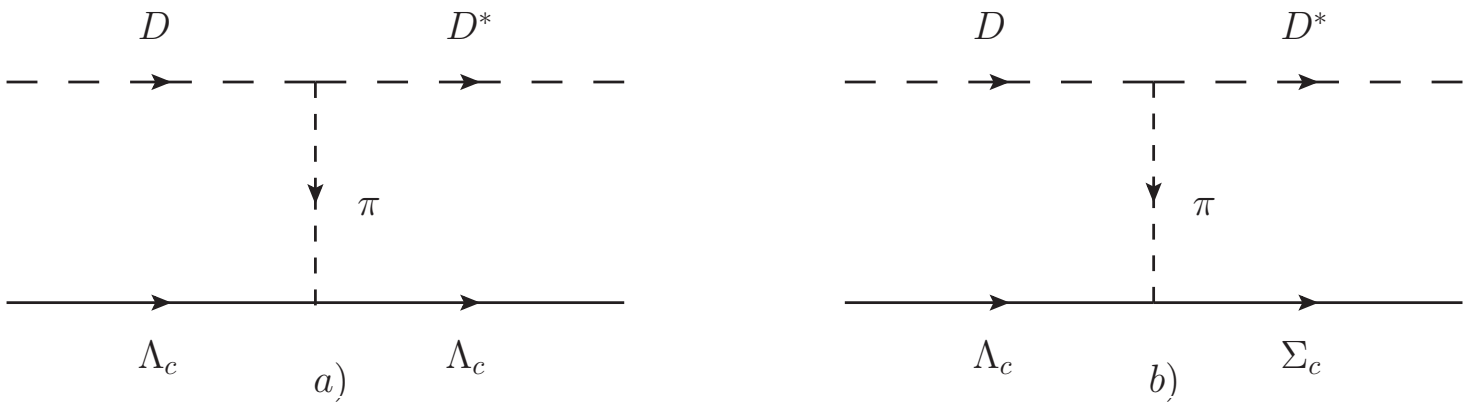


- C. W. Xiao, J. Nieves and E. Oset, PRD88,056012 (2013), evaluate the contribution of pion exchange, $\mu_{23}$, obtaining $\simeq 7\%$ (in the potential) of the $D\Lambda_c \to D\Lambda_c$ diagonal element.
- We also estimated the partial decay width of the $\bar{D}\Sigma_c$ molecular state $N^*_{c\bar{c}}$ to $J/\psi p$ through $t$-channel pseudoscalar $D^0$ exchange and found the partial width of $0.01$ MeV (about three orders of magnitude smaller than the decay to $\eta_c p$ (23.4 MeV) ) Phys. Rev. Lett. 105, 232001, J. J. Wu, R. Molina, E. Oset and B. S. Zou
- Similar results were obtained for the $D^{(*)}\bar{D}^{(*)}$ system in J. Nieves and M. P. Valderrama, PRD86,056004 (2012)

# Decay modes

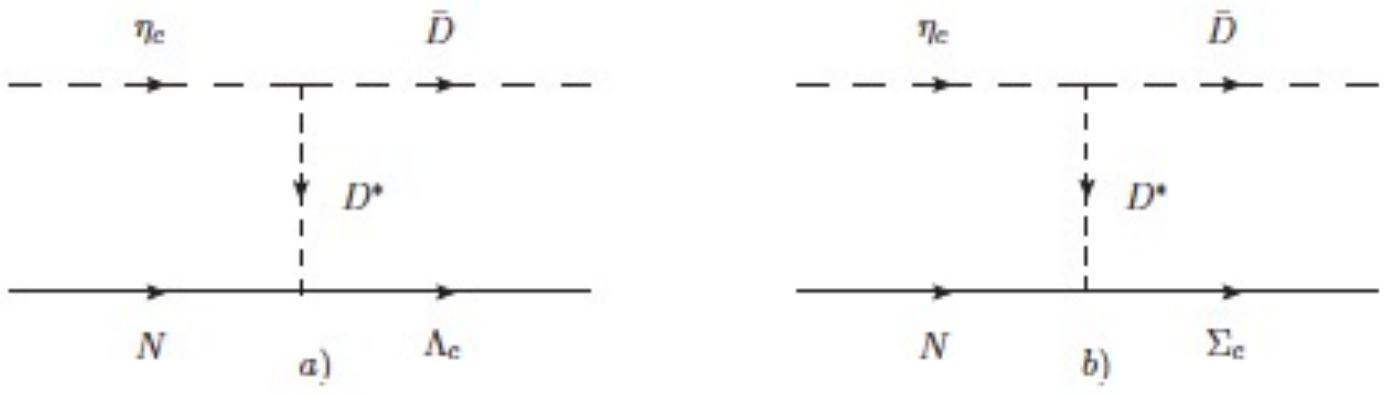


- The decay mode $\eta_c N$ or similarly, $J/\psi N$, is mediated by $D^*$. This term goes like $\mathcal{O}(1/m_{D^*}^2)$ and vanishes in the limit of $m_Q \to \infty$. However, this term is kept when using hidden gauge lagrangians.

- Similar results to PRC84, 015202 (2011) (J. J. Wu, R. Molina, B. S. Zou and E. Oset) are obtained in the work of C. W. Xiao, J. Nieves and E. Oset, PRD88,056012 (2013), but also other states consequence of HQSS are obtained.

| | | | | | | | |
|---|---|---|---|---|---|---|---|
| | | | $4261.87 + i17.84$ | | | | |
| | $\eta_c N$ | $J/\psi N$ | $\bar{D}\Lambda_c$ | $\bar{D}\Sigma_c$ | $\bar{D}^*\Lambda_c$ | $\bar{D}^*\Sigma_c$ | $\bar{D}^*\Sigma_c^*$ |
| $\lvert g_i \rvert$ | 1.05 | 0.76 | 0.02 | 3.13 | 0.50 | 0.75 | 0.32 |
| | | | $4410.13 + i29.44$ | | | | |
| | $\eta_c N$ | $J/\psi N$ | $\bar{D}\Lambda_c$ | $\bar{D}\Sigma_c$ | $\bar{D}^*\Lambda_c$ | $\bar{D}^*\Sigma_c$ | $\bar{D}^*\Sigma_c^*$ |
| $\lvert g_i \rvert$ | 0.38 | 1.44 | 0.18 | 0.20 | 0.20 | 3.10 | 0.51 |
| | | | $4481.35 + i28.91$ | | | | |
| | $\eta_c N$ | $J/\psi N$ | $\bar{D}\Lambda_c$ | $\bar{D}\Sigma_c$ | $\bar{D}^*\Lambda_c$ | $\bar{D}^*\Sigma_c$ | $\bar{D}^*\Sigma_c^*$ |
| $\lvert g_i \rvert$ | 1.15 | 0.72 | 0.19 | 0.10 | 0.12 | 0.11 | 2.93 |

Table 11. Coupling constants of all channels corresponded to the poles in the $J = 1/2,\ I = 1/2$ sector found in PRD88,056012.

| | | | | | |
|---|---|---|---|---|---|
| | | $4334.45 + i19.41$ | | | |
| | $J/\psi N$ | $\bar{D}^*\Lambda_c$ | $\bar{D}^*\Sigma_c$ | $\bar{D}\Sigma_c^*$ | $\bar{D}^*\Sigma_c^*$ |
| $\lvert g_i \rvert$ | 1.32 | 0.28 | 0.52 | 2.99 | 0.80 |
| | | $4417.04 + i4.11$ | | | |
| | $J/\psi N$ | $\bar{D}^*\Lambda_c$ | $\bar{D}^*\Sigma_c$ | $\bar{D}\Sigma_c^*$ | $\bar{D}^*\Sigma_c^*$ |
| $\lvert g_i \rvert$ | 0.53 | 0.11 | 2.81 | 0.16 | 0.52 |
| | | $4481.04 + i17.38$ | | | |
| | $J/\psi N$ | $\bar{D}^*\Lambda_c$ | $\bar{D}^*\Sigma_c$ | $\bar{D}\Sigma_c^*$ | $\bar{D}^*\Sigma_c^*$ |
| $\lvert g_i \rvert$ | 1.05 | 0.20 | 0.16 | 0.22 | 2.86 |

Table 12. The coupling constants to various channels for certain poles in the $J = 3/2,\ I = 1/2$ sector found in PRD88,056012.

# Quantum numbers of the pentaquark $P_c(4450)$

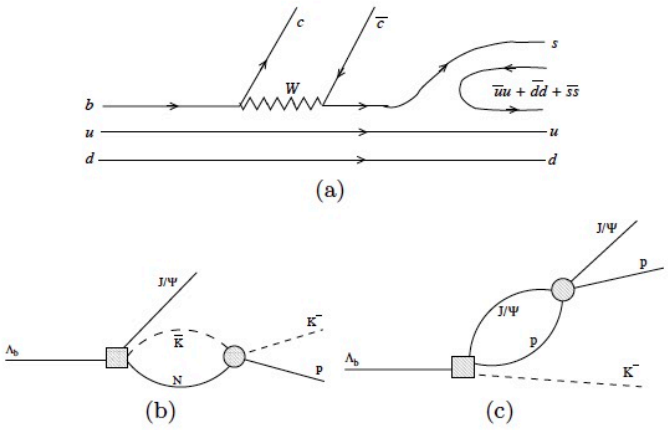


FIG. 1: Mechanisms for the $\Lambda_b \to J/\psi K^- p$ reaction implementing the final state interaction

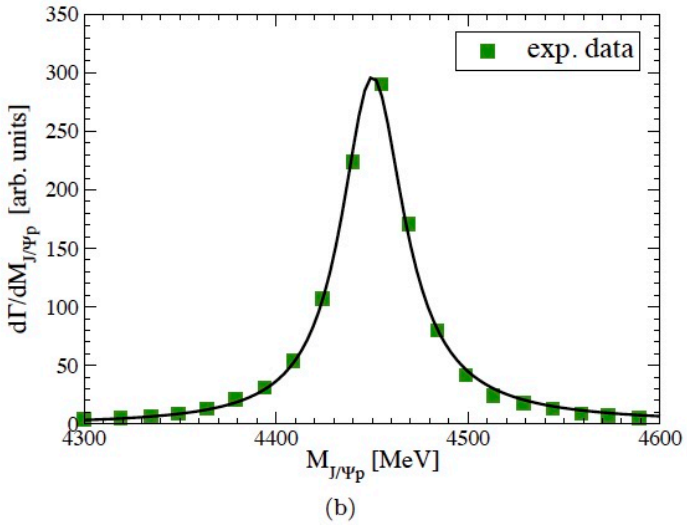


FIG. 2: Results for the $K^- p$ and $J/\psi\, p$ invariant mass distributions compared to the data of ref. [24].

The theoretical analysis of the $\Lambda_b \to J/\psi K^- p$ reaction is done by L. Roca, J. Nieves and E. Oset, PRD92, 094003(2015) supports the $J^P = 3/2^-$ assignment of the pentaquark state, and its nature as $\bar{D}^* \Sigma_c$, $\bar{D}^* \Sigma_c^*$ molecule.

# Conclusions

- The observed pentaquark by LHCb is a natural candidate to be a $\bar{D}^*\Sigma_c$, $\bar{D}^*\Sigma_c^*$ molecule with quantum numbers $J^P = 3/2^-$.
- Other states are expeced in the sector $I = 0, S = -1$ and masses $\simeq 4.4$ MeV decaying to $J/\psi\Lambda$ are predicted.
- Molecular states of $\bar{D}\Sigma_c$ decaying to $\eta_c N$ are expected (HQSS).
- These states can be also produced at FAIR in $p\bar{p}$ collisions.

## Inclusion of spin-1 fields

How to include vector fields in effective Lagrangians?

| | Yang-Mills | Hidden symmetry | WCCWZ | EGPdR |
|---|---|---|---|---|
| field formalism | vector | | | tensor |
| origin | gauge boson | | not gauge boson | |
| chiral realization | linear | non-linear and homogeneus | | |

**Table :** Essential features of different models to account for vector meson fields

# The hidden gauge formalism

Starting from a nonlinear sigma model based on $G/H = SU(2)_L \otimes SU(2)_R/SU(2)_V$: Bando,Kugo,Yamawaki

$$L = (f_\pi^2/4)\mathrm{Tr}(\partial_\mu U \partial^\mu U^\dagger)\ , \qquad U(x) = \exp[2i\pi(x)/f_\pi] \tag{17}$$

and introduce new variables $\xi_L, \xi_R$ and the field $V_\mu$:

$$U(x) \equiv \xi_L^\dagger(x)\xi_R(x)\ , V_\mu = (1/2i)(\partial_\mu \xi_L \cdot \xi_L^\dagger + \partial_\mu \xi_R \cdot \xi_R^\dagger) \tag{18}$$

Any linear combination $L = L_A + aL_V$ of the invariants:

$$L_V = -\frac{f_\pi^2}{4} Tr(D_\mu \xi_L \cdot \xi_L^\dagger + D_\mu \xi_R \cdot \xi_R^\dagger)^2 \quad L_A = -\frac{f_\pi^2}{4} Tr(D_\mu \xi_L \cdot \xi_L^\dagger - D_\mu \xi_R \cdot \xi_R^\dagger)^2$$

is equivalent to the original one, Eq. (17). A kinetic term is added, $-(1/4g^2)(V_{\mu\nu})^2$, and choosing $a = 2$ it is obtained

- 1)$m_\rho^2 = 2g_{\rho\pi\pi}^2 f_\pi^2$ (KSFR relation)
- 2)$\rho$ dominance of the electromagnetic form factor of pions $(gV_\mu(\pi \times \partial^\mu \pi))$

And, fixing the gauge $\xi_L^\dagger = \xi_R \equiv \xi$ the Lagrangian becomes in the Weinberg's Lagrangian (nonlinear realization of the chiral symmetry)

# Inclusion of spin-1 fields

$$
\begin{aligned}
V_{\mu\nu} &= \partial_\mu V_\nu - \partial_\nu V_\mu - ig[V_\mu, V_\nu] \\
\Gamma_\mu &= \frac{1}{2}[u^\dagger(\partial_\mu - ieQA_\mu)u + u(\partial_\mu - ieQA_\mu)u^\dagger] \qquad u^2 = U
\end{aligned} \tag{19}
$$

$$
\frac{F_V}{M_V} = \frac{1}{\sqrt{2}g}, \qquad \frac{G_V}{M_V} = \frac{1}{2\sqrt{2}g}, \qquad F_V = \sqrt{2}f, \qquad G_V = \frac{f}{\sqrt{2}}, \qquad g = \frac{M_V}{2f} \tag{20}
$$

Upon expansion of $[V_\mu - \frac{i}{g}\Gamma_\mu]^2$

$\mathcal{L}'s$

$$
\begin{aligned}
\mathcal{L}_{V\gamma} &= -M_V^2 \frac{e}{g} A_\mu \langle V^\mu Q \rangle \\
\mathcal{L}_{V\gamma PP} &= egA_\mu \langle V^\mu (QP^2 + P^2 Q - 2PQP) \rangle \\
\mathcal{L}_{VPP} &= -ig \langle V^\mu [P, \partial_\mu P] \rangle \\
\mathcal{L}_{\gamma PP} &= ieA_\mu \langle Q[P, \partial_\mu P] \rangle \\
\widetilde{\mathcal{L}}_{PPPP} &= -\frac{1}{8f^2} \langle [P, \partial_\mu P]^2 \rangle .
\end{aligned} \tag{21}
$$